

Self-pulsating semiconductor lasers for high bit-rate all-optical clock recovery

P. Gallion^a, J. Renaudier^{a,b}, G.-H. Duan^b, and B. Lavigne^c

^aEcole Nationale Supérieure des Télécommunications, CNRS LTCI UMR 5141
46, rue Barrault, 75634 Paris Cedex 13, France

^bAlcatel Thales III-V Laboratory, Route Départementale 128, 91767 Palaiseau, France

^cAlcatel Research & Innovation, Route de Nozay, 91460 Marcoussis, France

ABSTRACT

Clock recovery using self pulsating semiconductor laser structure is a sophisticated signal processing inside the device, involving optical injection locking, gain and index modulation, self pulsation, radiofrequency oscillation synchronization, and phase noise filtering. The mutual injection of the longitudinal mode and the passive mode locking leading to self pulsation is analyzed by using multimode rate equations. Self pulsation is easily achievable and is characterized by a large reduction of the RF spectral line width, as compared to those of the optical modes involved in the beating process. When they are injected by a power modulated optical signal, the self pulsating laser structures act as all-optical clock recovery devices. The self pulsation line width is found to be determinant to fulfill the high bit-rate optical communications and optical signal processing clock recovery property requirement.

Keywords: Optical clock recovery, self pulsation, mode locking, four wave mixing, phase noise, jitter, injection locking.

1. INTRODUCTION

Clock agreement has been recognized early as one of the more difficult tasks. In the 16th century, when retired from the greatest throne in the world, the King of Spain was declaring [1]:

*“To think that I attempted to force the reason and conscience of thousands of men into one mold,
and I cannot make two clocks agree!”* Charles Quint (1500-1558)

In any digital signal communication or processing systems, the clock recovery is a key element, for decision or regeneration. For instance, clock recovery at 40 Gbit/s and beyond is required for the future transparent optical networks. Optoelectronic hybrid clock recovery schemes, including a high speed photo-receiver, a high-Q filter, a power electrical amplifier and a laser with an integrated modulator appears as a too complex solution, with the additional well known drawback of optical to electrical conversion. All-optical signal processing such as all-optical digital logic functions and 3R (Retiming, Reshaping and Reamplifying) regenerators require truly all-optical clock recovery at very high bit rate, in order to improve the transmission distance, the transparency, the capacity and the speed of optical networks.

A self-pulsation (SP) regime of semiconductor lasers is a regime in which one observes a periodic variation of the output power of the laser even though it is DC biased. Various semiconductor laser structures exhibit self pulsating operation, including Fabry-Perot (FP) [2, 3], distributed feedback (DFB) [4, 5] and distributed Bragg reflectors lasers (DBR) [6, 7]. All these structures have been already studied for clock recovery at 40 Gbit/s. The latter offers operating advantages such as large SP regime range and tunability of the emitted wavelength.

More specifically for DBR lasers, a self pulsating oscillation at frequencies up to 500 GHz has been reported in such lasers including a saturable absorber. In this case the SP originates from passive self Q-switching due to the modulation of absorption [5, 8]. In DBR lasers without saturable absorber, the beating between the longitudinal modes generates a

optical power oscillation under appropriate bias conditions. All-optical clock recovery up to 240 Gbit/s [7, 9, 10] has been demonstrated with both types of SP DBR structure.

Clock recovery using SP structure is a sophisticated signal process inside the device, involving optical injection locking, gain and index modulation, self pulsation, RF oscillation synchronization, phase noise filtering. The aim of this paper is to review these optical and RF signal process, to discuss the involved physical effects and to present their modeling tools. Achievable performance and experimental results at 43Gbit/s using bulk, quantum well (QW) and quantum dot (QD), DBR and FP 1.5 μm laser structures are reported. The paper is organized as follows. The second section is devoted to the longitudinal mode injection locking and the passive mode locking leading to self pulsation. Physical origin, theoretical analysis using multimode rate equations, and experimental results are reported. The optical phase correlation and self pulsation phase noise, determinant for the recovered clock properties, are discussed in the third section. The self pulsating line width is at the same time the manifestation of the mode correlation and the key parameter for clock recovery application which is discussed in the third section.

2. PASSIVE MODE LOCKING BY MUTUAL INJECTION

2.1. The self pulsation origin

Under standard operation condition a multimode semiconductor laser is not self-pulsating because its longitudinal modes are not equally spaced, thanks to group index and effective length dispersion. Furthermore, the modes are usually only coupled by the phase insensitive gain saturation process, and each of them undergoes an independent and meaningless average phase Wiener-Lévy diffusion process. In this condition, there is no coherent interaction between the modes and a continuous optical power out put, resulting of their powers addition, is usually observed.

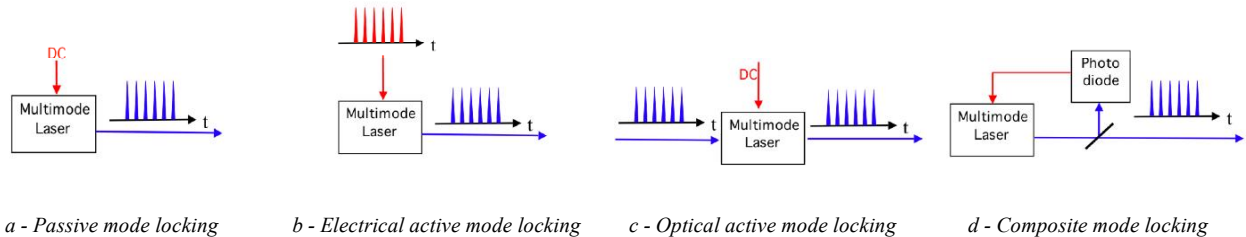


Figure 1: Active and passive mode locking mechanism

A SP regime is usually considered as spurious and may be eventually ignored as far as low power modulation frequency are involved. The longitudinal modes beating, or more exactly the modulation at their frequency spacing is the key phenomena to achieve self pulsating operation by passive mode locking (Fig 1a). The active mode locking of a semiconductor laser structure may be achieved by direct electrical modulation of the driving current at a frequency close to longitudinal mode frequency spacing (Fig 1b). It may also be produced, under constant electrical current injection, by the modulation of the carrier population by injection of an external modulated optical signal (Fig 1c). Mode locking may be also achieved by electrical driving of the laser by the self pulsating power detection current (Fig 1d). Since the carrier density modulation at the self pulsating frequency can be directly obtained in the passive mode locking configuration, this last scheme, which is difficult to implement due to optoelectronics integration problems, will not be discussed here despite its fundamental interest.

The origin of SP in multimode semiconductor lasers without saturable absorber is usually attributed to nonlinear mechanisms of interaction between the modes in the gain region [11, 12]. In semiconductor lasers four wave mixing (FWM) associated to mutual side band injection locking is well known to be the phase sensitive phenomenon equaling the frequency difference between modes and introduced their phase correlation [13, 14, 15]. Four wave mixing (FWM) may also usually be referred as modulation side band generation induced by gain and optical index pulsation, or as third order inter modulation [16]. A minimum of three modes is to be considered for FWM interaction.

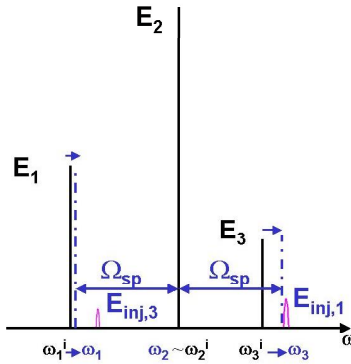


Figure 2: Schematic description of mutual injection regime through modulation side bands, leading to passive modes locking

Let us consider a three longitudinal mode operation as displayed on Figure 2. The fields associated to the side modes E_3 and E_1 induce their own symmetrical fields E_{inj1} and E_{inj3} with respect to the central mode E_2 . The field E_{inj1} and E_{inj3} are respectively within the injection locking bandwidth. They act as frequency pulling or pushing effects on ω_1^i and ω_3^i similar to those describing an externally injection-locked laser. The only difference with external injection locking phenomenon is that the injection optical fields are self-generated inside the laser cavity.

2.2. Basics of injection locking

Injection locking only occurs when the frequency difference between the injected field and initial mode falls within the locking range, which depends on the amount of injected power as well as the phase-amplitude coupling in the cavity of the injected laser [17, 18, 19]. The general discussion on the locking of RF or gas laser oscillators is to be adapted to the case of semiconductor laser by including phase-amplitude coupling effect [20].

The coherent addition, to a preexisting field with amplitude E and relative phase ϕ , of a weak injected optical field, with amplitude E_i and relative phase $\theta = \phi_{in} - \phi$, (Fig 3), produces a direct phase change $\Delta\phi = (E_i \sin\theta)/E$ and an amplitude change $\Delta E = E_i \cos\theta$. The gain saturation process, restoring initial amplitude, produces in turn a phase-amplitude coupling induced additional phase change $\Delta\phi' = \alpha_H (E_i \cos\theta)/E$ [21, 22, 23]. The phase-amplitude coupling is represented by the factor α_H .

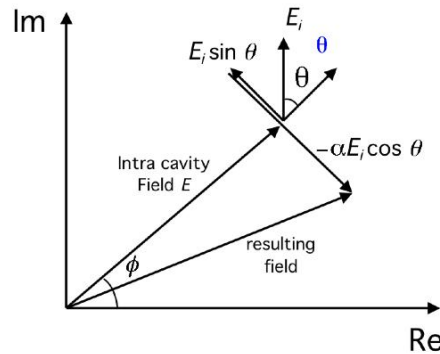


Figure 3: Injection induced amplitude change and direct and indirect phase changes

Considering a cold cavity resonator with quality factor Q , the phase ϕ of the locked oscillator is governed by the generalized Adler's equation

$$\frac{d\phi}{dt} = -\Delta\omega + \frac{\omega}{2Q} \frac{E_i}{E} (\sin\theta - \alpha_H \cos\theta) \quad (1)$$

where $\Delta\omega$ is the angular frequency detuning between the free running and the injection locked oscillations. In a steady state regime, the angular frequency detuning counter-acts the total phase change per unit of time induced by injection and we have

$$\Delta\omega = \Delta\omega_{LOCK} \sin(\theta - \arctan\alpha_H) \quad (2.)$$

where the locking range $\Delta\omega_{LOCK}$ of the oscillator is the maximum achievable angular frequency change and is given by

$$\Delta\omega_{LOCK} = \frac{\omega}{2Q} \frac{E_{inj}}{E} \left(1 + \alpha_H^2\right)^{1/2} \quad (3.)$$

For a given value of the detuning $\Delta\omega$, θ is constant, meaning that phase difference between the injected and the locked signal is kept constant.

The phase-amplitude coupling factor α_H induces an enhancement of the maximal detuning between the initial frequencies. The locking range depends also on the relative power between modes involved through injection rate terms. Indeed, the stronger the modulation side band, the larger is the possible frequency shift of the injected mode. When the locking is obtained the SP frequency Ω_{sp} is close to the mode-spacing frequency.

2.3. Rate equations modeling

To study mode locking, we use standard multimode rate equations including self-induced carrier density modulation [24, 25]. The coupled mode equations, describing PML enables the study of the evolution in amplitude and phase of longitudinal modes under the usual slowly varying wave approximations

$$\frac{d}{dt} E_k = \underbrace{\frac{1}{2}(1 - j\alpha_H)(G - \gamma_k)E_k}_{\text{Linear gain and loss}} + \underbrace{\frac{1}{2}(1 - j\alpha_H) \frac{\Gamma C v_g \alpha}{V} \left[\sum_{m=1}^{M-1} (\Delta N_m E_{k-m} + \Delta N_m E_{k+m}) \right]}_{\text{Carrier density modulation}} - \underbrace{j(\omega_k - \omega_k^i)E_k}_{\text{Angular frequency detunning}} + \underbrace{F_k(t)}_{\text{Langevin noise force}} \quad (4.)$$

where α_H represents the phase-amplitude coupling factor, γ_k the cavity loss for the k th mode. The instantaneous fluctuations of the electric field are given by Langevin source term, $F_k(t)$. $(\omega_k - \omega_k^i)$ represents the detuning of the angular frequency lasing mode away from its initial cavity resonance one. The gain, G is assumed constant over the spectral range of the three considered modes. G is given by $\Gamma v_g g$ with Γ the optical confinement, v_g , the group velocity and g expressed as $a(N_0 - N_{tr})/V$, where a is the differential gain, V the volume of the active layer, N_{tr} , the carrier number at transparency, N_0 the average carrier number, satisfying the carrier rate equation given by:

$$\frac{dN_0}{dt} = \frac{I}{e} - \frac{N_0}{\tau_e} - GP_t \quad (5.)$$

Where P_t is the total photon number i.e. the sum of the squared fields of the active modes. ΔN_m represents the m th order carrier modulation given by

$$\Delta N_m = -(N_0 - N_{tr}) \frac{\sum_{i=1}^M E_k E_{i-m}^*}{P_t + P_s - jm\Omega_{sp}\tau_e P_s} \quad (6.)$$

with the photon saturation number, P_s equals to $V/(G\tau_e)$, and τ_e the carrier lifetime. Since $\Omega_{sp}\tau_e \gg 1$, the contribution of $(1 + P_t/P_s)$ to the carrier modulation can be neglected. Detailed analysis is beyond the scope of this paper and has extensively been published. Neglecting the transfer of energy between modes by the non-linear gain, the contribution of the non-linear gain is only the introduction of a phase coupling. As observed in the experiment reported below, we consider three longitudinal modes propagating inside the cavity with mode-spacing Ω_{sp} and we consider that the amplitude of the side mode 2 is larger than the one of the main mode 1, which is larger than the one of the side mode 3.

2.4. Self pulsation operation condition

Solving these equations for a steady-state analysis, it was possible to determine the criteria to achieve the self-pulsation. When the initial angular frequency mismatch exceeds a limit value, passive mode locking cannot be achieved. When

one of the side-modes is stronger than the other, the locking strength increases to induce a larger frequency shift of the last one, as shown in Fig 4. This figure also shows that, by increasing the photon density inside the cavity (expressed by the ratio A_2^2/P_s , where A is the mode amplitude), the locking bandwidth easily becomes larger than 100 MHz for any injection power rate.

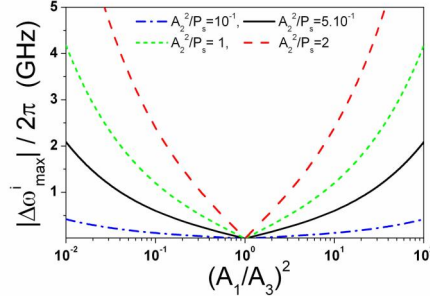


Figure 4: Maximum allowed frequency mismatch as a function of the ratio of power injected in mode 1 and 3, for different values of the photon density inside the cavity expressed by A_2^2/P_s

Considering a free spectral range in the order of 40 GHz for our DBR lasers, such values of locking bandwidth explain why SP appears as soon as the output power reaches 1mW in our DBR lasers. Therefore, such a result demonstrates that self-pulsation at 40 GHz is easily achieved in DBR semiconductor lasers because interband effects are sufficiently important to induce natural occurrence of passive mode-locking for usual amounts of power.

2.5. Experimental results

We will present below as an example, the self pulsating behavior of one of the three different laser structures investigated in this paper. It is a multiple quantum well distributed Bragg reflector (DBR) lasers that consists of three sections: active, phase and Bragg [15]. It has a short Bragg section of 150 μm allowing to have mainly 3 longitudinal modes. The active section is 900- μm -long and consists of nine quantum wells and eight barriers of thickness of 8 nm and 10 nm respectively, surrounded by two separated confinement heterostructure guiding layers of total thickness of 200 nm. Under broad bias conditions, such a DBR laser operates typically in a multimode regime allowing the existence of self-pulsation by longitudinal mode beating. Fig. 5 shows a typical evolution of SP frequency as a function of the active current for such DBR lasers. We observe on this figure the rapid occurrence of SP at frequencies close to 40 GHz. We also see some SP frequency jump induced by the typical phenomenon of mode-hopping in multimode DBR lasers.

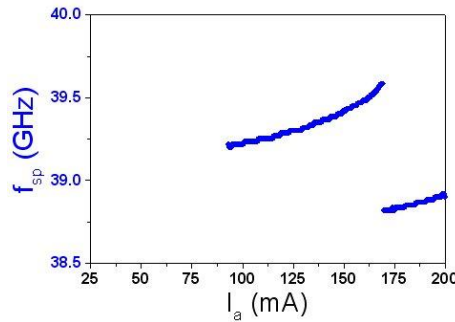


Figure 5: Evolution of the SP frequency as a function of the active current.

3. OPTICAL PHASE CORRELATION AND SELF PULSATION PHASE NOISE

3.1. From mode optical line width to RF self pulsating line width

Discarding the deterministic term $\Omega_{sp} t$, the instantaneous phase of the beating signal between the modes i and k is related to mode phase noises $\phi_i(t)$ and $\phi_k(t)$ by

$$\phi_{ki}(t) = \phi_k(t) - \phi_i(t) \quad (7.)$$

For completely independent modes the power spectral density (PSD) of frequency noise for the optical beating is the sum of their independent spectral densities of frequency noise

$$S_{\phi_{ki}}(\omega) = S_{\phi_k}(\omega) + S_{\phi_i}(\omega) \quad (8.)$$

Because frequency noise is the formal time derivative of phase noise, and we have

$$S_{\dot{\phi}}(\omega) = \omega^2 S_{\phi}(\omega) \quad (9.)$$

and a similar relation to Eq.7 holds for the PSD of frequency noise

$$S_{\dot{\phi}_{ki}}(\omega) = S_{\dot{\phi}_k}(\omega) + S_{\dot{\phi}_i}(\omega) \quad (10.)$$

The phase-amplitude coupling factor is another mechanism providing phase correlation. Under spontaneous emission fluctuation each mode undergoes amplitude and directly induced phase changes. Through phase amplitude coupling the gain changes correcting amplitude fluctuation induced indirect index change. However, each mode experiences the same indirect index change turning into the same phase change. The mode locking process previously described only acts as a restoring force for the phase diffusion produced only by the directly induced phase change. Using these two phenomena, a complete phase correlation between the modes is in principle achievable. Under practical condition only partial correlation is obtained and the power spectral density of frequency noise for the optical beating fulfills

$$S_{\dot{\phi}_{ki}}(\omega) < S_{\dot{\phi}_k}(\omega) + S_{\dot{\phi}_i}(\omega) \quad (11.)$$

We assume negligible $1/f$ carrier noise contribution and therefore Lorentzian shape for longitudinal modes and beating RF spectrum. In this case PSD of frequency noise is flat for low frequencies and the spectral line width is given by

$$\Delta\nu = \frac{\Delta\omega}{2\pi} = \frac{S_{\dot{\phi}}(0)}{2\pi} \quad (12.)$$

From a small-signal analysis, starting from Eq. 3, it is possible to extract the PSD of relative phases ϕ_{21} and ϕ_{32} and to study the stability of the solution. Fig. 6 shows the frequency noise PSD of the relative phases, and the sum of frequency noise PSD for longitudinal modes. The solid curves describe the frequency noise spectra related to the beating between modes 1 and 2, and the dashed ones describe the frequency noise spectra related to the beating between modes 2 and 3. We observe a large reduction of PSD of the relative phases from that of the sum of frequency noise PSD of longitudinal modes for low analysis frequencies. We of course observe relaxation oscillation peak at a frequency of 9 GHz.

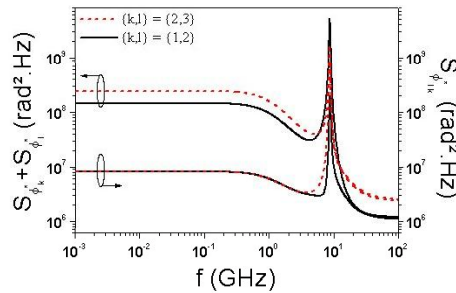


Figure 6: FM noise spectra for the relative phases ϕ_{21} and ϕ_{32} , as compared to the sum of FM noise spectra for longitudinal modes

3.2. Optical line width and RF self pulsating line width measurement

Fig. 7 shows a typical optical spectrum the three sections multiple quantum wells distributed Bragg reflector laser, showing that the laser nearly operates in a three-modes regime: the fourth mode is at least 10 dB lower than the third one. The RF beating spectrum is the superposition of the two main to side mode beatings while the side to side mode beating produces the second harmonic.

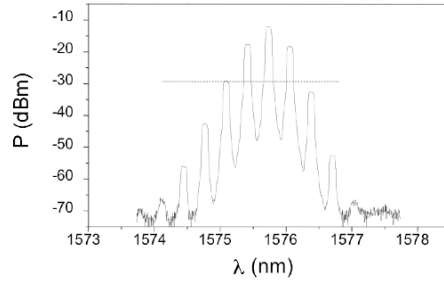


Figure 7: Typical optical spectrum the three sections multiple quantum wells distributed Bragg reflector laser

To observe the RF beating spectrum the optical beam is detected under standard conditions and resulting photocurrent is observed with an electrical spectrum analyzer (ESA) with a span of 18 MHz and a resolution bandwidth of 300 kHz. The radio-frequency (RF) spectrum of the photocurrent is a Lorentzian shape centered at the self pulsating frequency and the measured line width is the full width half maximum (FWHM) of this RF signal which is in the few hundred-kHz range. To investigate more in details the composite the beating process we have isolated the two beating components at the mode-spacing frequency that constitute the SP signal. By using a monochromator, which acts as an optical tunable band pass filter, setting the filtering band pass to 0.5 nm, the monochromator enables the selection of two optical modes and the observation of their own contribution to the beating. The line widths have been found to be identical for the 2 beatings and in a range of few hundreds kHz, which shows that the correlation level between phases of modes 1 and 2 is the same as that between phases of modes 2 and 3.

To allow comparison with the individual optical line width of the modes, the longitudinal modes are individually filtered; by setting the band pass of the monochromator to 0.1 nm, in order to measure their spectral line widths, using a self-homodyne technique. Fig.8 shows the spectral line widths of longitudinal modes and auto pulsating (AP) signal with an increasing injected current the Bragg section of the DBR laser, until a mode jump occurs. The spectral line widths of the longitudinal modes decrease with increasing current, due to the decrease of the effective phase-amplitude coupling factor. The line width of the RF signal is affected by the increase of Bragg current and follows the decrease of the line widths of the longitudinal modes. The line width of SP signal is always much narrower than that of the longitudinal modes as in FP semiconductor lasers. Such a result demonstrates that the phase of each longitudinal mode fluctuates upon spontaneous emission, leading to the line width measured of the order of several tens of megahertz. However, the reduced line width of the SP signal, of the order of megahertz, shows that these fluctuations are largely synchronized [15].

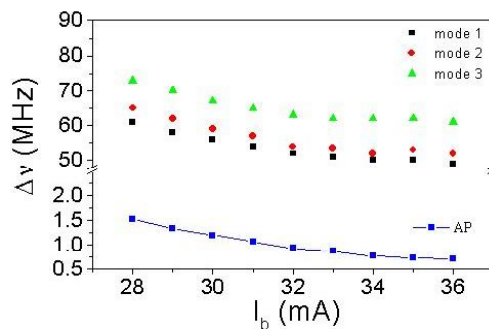


Figure 8: Spectral line widths of the 3 longitudinal modes and of the auto pulsating (AP) signal as a function of the current injected the Bragg section of a 6 quantum well DBR laser

Line width measurement of the self pulsating spectrum has been performed on two other self pulsating laser structures. The second one is a 3 sections DBR laser. The active section has a length of 790 μm . The guiding layer is a bulk quaternary material with a thickness of 0.4 μm and a width of 0.6 μm . Such a quasi-square cross-section allows obtaining a polarization-insensitive modal gain. In the phase section of a length of 130 μm , the width of the waveguide expands

linearly to match the 1.8 μm wide Bragg section. The short 200 μm -long Bragg section enables to have at least two longitudinal modes inside the 3dB bandwidth of the Bragg reflection spectrum.

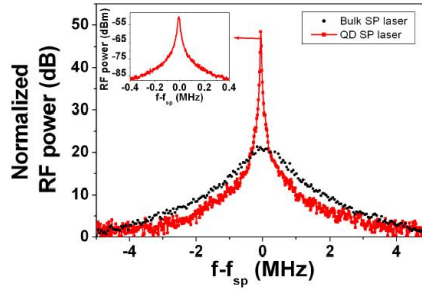


Figure 9: Comparison of the self pulsating RF spectra obtained in the case of bulk DBR laser (straight line) and of QD laser (dotted line).

The third studied semiconductor lasers are made of a buried ridge structure, and contain an active layer based on QD on InP substrate. The QD-based heterostructure was grown by GSMBE on an S-doped (100) InP wafer. The active core consists of 6 layers of InAs QD enclosed within 40nm-thick barriers and two 40nm-thick separate confinement heterostructure (SCH) layers. Both barriers and SCH are undoped and lattice-matched Ga_{0.2}In_{0.8}As_{0.4}P_{0.6} layers ($\lambda_g=1.17\mu\text{m}$). The typical height and diameter of QD are 2.3nm and 20nm, respectively. The density of dots per QD layer is about $2 \times 10^{10} \text{ cm}^{-2}$. Both facets are cleaved, forming a Fabry-Perot (FP) cavity. The studied FP laser has a cavity length of 950 μm .

Fig. 9 shows the comparison of the self pulsating RF spectra obtained for these bulk DBR laser and of QD laser structure. Self-Pulsation at 45 GHz in the 1.5- μm monolithic single-section quantum dots Fabry-Perot semiconductor lasers without saturable absorber exhibits a mode-beating narrow linewidth of about 20 kHz, demonstrating high phase correlation between these modes. The self pulsating line width observed for bulk DBR laser is close to 1MHz.

4. SELF PULSATION LOCKING AND OPTICAL CLOCK RECOVERY

4.1. Jitter in digital systems and clock recovery

Jitter is a fast noise manifestation in the temporal domain. Jitter manifestation is deviations $\delta\tau$ of “significant instants”, such as transitions edges in a digital signal, from their nominal position. Assuming a signal with average angular frequency f_0 , time positioning fluctuation jitter $\delta\tau$ appear as a consequence of phase noise $\delta\phi(t)$ related by

$$\delta\phi(t) = 2\pi f_0 \delta\tau(t) \quad (13.)$$

Jitter basically differs from slow variations that are called drift or wander which are easily eliminated at the emission and are not generated by non linear and dispersive propagation.

Jitter is a random process and is to be treated and characterized in terms of its statistics moments. Its mean value is usually equal to zero and its peak-to-peak value is dependent on the observation duration. The two-sided power spectral densities of phase noise $S_\phi(f)$ and time fluctuation noise $S_\tau(f)$ are related by

$$S_\phi(f) = (2\pi f_0)^2 S_\tau(f) \quad (14.)$$

Under Gaussian assumption it usual to characterize jitter by its standard (i.e. r.m.s.) deviation whose square value is related to the power spectral density phase of noise S_ϕ by

$$\sigma^2 = \frac{1}{(2\pi f_0)^2} \int_{-\infty}^{+\infty} S_\phi(f) df \quad (15.)$$

Jitter turns into bit error rate (BER) because decision is usually made on these “significant instants” when the transitioning signal crosses a chosen decision threshold which is up to now an optical intensity level. Furthermore, in the

case of data modulated with a non-return-to-zero modulation format, since no transition may occur when the same bit is repeated two or more times, the number of a given transition into a bit duration have only a maximum value of one. An ideal clock is the corresponding periodic signal, for instance the sine signal, containing exactly one leading edge and one trailing edge at their nominal position in each bit duration and allowing ideal position definition and decision. Since an ideal clock is not already available at the end of an optical transmission line an *optical clock recovery* is required. The optical clock recovery is the signal processing for establishing the reference clock from the transmitted signal, that will be used for decision or signal inline regeneration. A standard effective method of clock recovery is the use of a phase locked loop (PLL) [26,] tracking slowly varying changes in the symbol rate of the measured data. Consequently, it acts as a low-pass filter with respect to the jitter that remains on the output signal. The jitter suppression effect of the all-optical clock recovery is analyzed through phase noise measurements.

4.2. Locking of the self pulsating oscillation

In this section the self pulsating laser is no more considered as an optical oscillator but as a radiofrequency one for which the oscillating parameter is the optical power $P(t)$. As depicted in Fig.10a this oscillator is locked by the power modulation of an injected optical signal. The launched optical signal only modulates the carrier density and does not play any other role in the locking process [27]. An additional cooperative effect may be included by electrical driving of the laser by self pulsating power detection current (Fig 10d) but will not be discussed here.

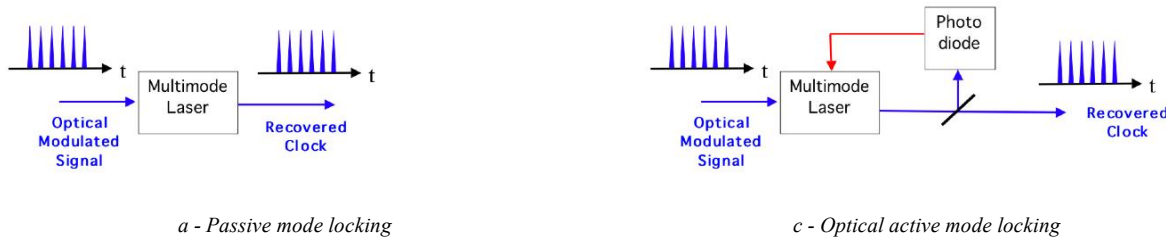


Figure 10: Active and passive mode locking mechanism

As for any oscillators, the injection locking occurs when the frequency difference between the injected signal and the initial self pulsating signal falls within the locking range, which depends on the amount of injected signal power. No phase-amplitude coupling in the cavity of the injected laser has to be considered since the locking process does not involve the optical field but the optical power. The locking range of an oscillator with a quality factor Q is written as:

$$\Delta\omega_{LOCK} = 2\pi\Delta f_{LOCK} = \frac{\omega}{Q} \frac{P_{inj}}{P} \quad (16.)$$

Let us consider a self-pulsating laser at frequency f_{AP} . As experiments pointed it out, the self pulsation spectrum is well modeled by a Lorentzian line shape corresponding to a flat power spectral density frequency of noise and therefore to a power spectral density of phase noise $S\phi_{AP}$ which can be written as

$$S_{\phi_{AP}}(f) = \frac{\Delta\nu}{2\pi f^2} \quad (17.)$$

where $\Delta\nu$ is the full line width at half maximum (FWHM) of the free running self-pulsating signal. Let us consider now the optical injection of an optical clock at frequency f_{in} and having a power spectral density of phase noise $S\phi_{in}$. The synchronization of the self pulsation rate on the pulsation rate of injected optical signal is strongly dependent on the difference between the injected signal and the free running one $\Delta f = f_{in} - f_{AP}$.

The maximum value for which a frequency locking is obtained is the locking bandwidth Δf_{LOCK} meaning obviously that a wider spectrum is more sensitive to spectrally distant injection. It is to be mentioned that this optically supported radiofrequency injection is not an optical injection locking and that the phase amplitude coupling does not enhance the radiofrequency locking bandwidth. For a given value of the power of the injected signal, the smaller the free running line width, the smaller is the locking bandwidth.

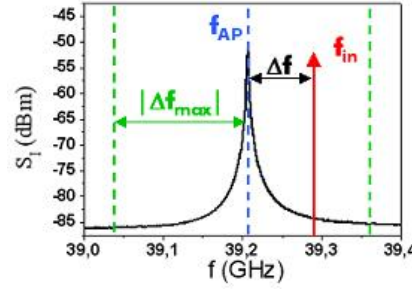


Figure 11: Free running spectrum and locking bandwidth

The standard rate equation for the phase ϕ_L of the locked self pulsating oscillation is expressed as :

$$\frac{d\phi_L}{dt} = 2\pi\Delta f + 2\pi\Delta f_{LOCK} \sin(\phi_{in} - \phi_L) + \dot{\phi}_{AP} \quad (18.)$$

where Δf is the frequency difference between the injected signal f_{in} and the free running self pulsation frequency f_{AP} . and Δf_{LOCK} the locking bandwidth. After linearization, considering each phase signal as the sum of a quiescent value and fluctuation, in the form

$$\phi(t) = \bar{\phi} + \delta\phi(t) \quad (19.)$$

and observing that the quiescent values fulfill the static equations

$$\Delta f = \Delta f_{LOCK} \sin(\bar{\phi}_{in} - \bar{\phi}_L) \text{ and } f_L = \Delta f_{LOCK} \cos(\bar{\phi}_{in} - \bar{\phi}_L) \quad (20.)$$

We obtain in the Fourier domain

$$(jf + f_L)\delta\phi_L(f) = f_L \cdot \delta\phi_{in}(f) + jf \cdot \dot{\phi}_{AP}(f) \quad (21.)$$

The power spectral density of phase noise S_{ϕ_L} of the locked self pulsation is classically obtained by the ensemble average

$$S_{\phi_L}(f) = \langle \delta\phi_L(f) \delta\phi_L^*(f) \rangle \quad (22.)$$

It depends on the PSD of phase noise $S_{\phi_{in}}$ of the injected signal and on the on the PSD of phase noise $S_{\phi_{AP}}$ of the free running self pulsation

$$S_{\phi_L}(f) = \frac{f_L^2}{f^2 + f_L^2} S_{\phi_{in}}(f) + \frac{f^2}{f^2 + f_L^2} S_{\phi_{AP}}(f) \quad (23.)$$

where the cutoff frequency f_L is given by

$$f_L = \sqrt{\Delta f_{LOCK}^2 - \Delta f^2} \quad (24.)$$

The cutoff frequency f_L is enlarged when the detuning of the injected signal is reduced and its maximum is the locking range.

For $f \ll f_L$, the synchronized self pulsation phase noise is governed by the injected signal phase noise and the device is transparent to injected noise. The device, introducing no input filtering, allows the tacking of the low frequency variation of the input clock.

For $f \gg f_L$, the synchronized self pulsation phase noise is governed by the free running self pulsation noise. The high frequency phase noise components of injected clock signal are rejected with an $1/f^2$ decay transfer function.

For f close to f_L , it is the transition region where the two contributions add and the resulting noise is larger than any one of them.

Usually optical injection locking is used to transfer the low frequency phase noise of a weak master to a powerful slave one. In the case of clock recovery, we are facing with the opposite problem that consist in rejecting the high frequency

phase noise of the injected signal to obtain a fluctuation filtering output containing only the low frequency components of the input signal. The above expression for the phase noise of the injection locked laser shows that it behaves as a second order filtering of the input phase noise with a -3dB cut-off frequency being the locking characteristic frequency equal to f_L . The second term represents the added phase noise contribution of the free running SP laser, acting as an active filter. The maximum value of the cut-off frequency for resonant injection ($\Delta f = 0$) and is equal to Δf_{LOCK} . There is great interest to obtain the lowest cut off frequency by minimizing Δf_{LOCK} . Δf_{LOCK} is reduced by enlarging the quality factor Q of the self pulsating oscillator. A high Q value is achieved with low self pulsating line width, which is a key issue for the high frequency rejection of the injected signal phase noise. However the price to pay is a reduction of the cut-off frequency for high pass filter for free running self pulsating phase noise.

4.3. Phase noise filtering

We have performed phase noise measurement by using the two previously described semiconductor lasers of a buried ridge structure. The first one is a Distributed Bragg Reflector (DBR) laser containing a bulk active layer. The second one is a single-section Fabry-Perot (FP) laser containing a QD active layer on InP substrate (100). The measurement is performed by adjusting the incoming jitter by using a 10 GHz external clock, provided by a synthesizer, whose jitter is monitored by a white noise generator (10kHz - 1GHz). An OTDM system delivers at last the 40 Gbit/s signal. With no PRBS data drive the OTDM delivers return-to-zero (RZ) data at 40 Gbit/s coded with pseudo-random bit sequences (PRBS) of $2^{31}-1$. Phase noise measurements are obtained with an Europtest jitter analyzer.

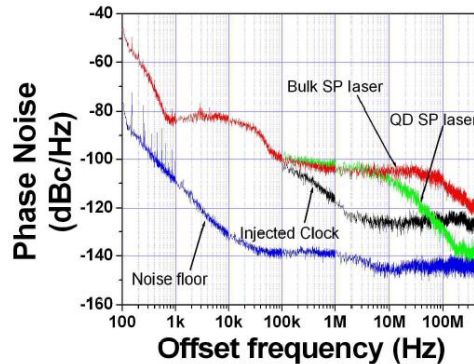


Figure 12: Phase noise spectra of the reference clock, the recovered clock from the Bulk SP laser and that from the QD SP laser. The lower spectrum indicates the noise floor of the apparatus.

Fig. 12 presents and compares the phase noise measurements performed with a bulk SP laser and a QD SP laser, along with the phase noise spectrum of the reference clock and the noise floor of the jitter analyzer. The reference clock corresponds to the clock signal that we use to carve the RZ data and that is delivered by the OTDM systems when no PRBS are used. For frequencies lower than 60 kHz, the phase noise from the injected clock signal dominates, corresponding to the so-called transparent region in which the injected clock fluctuations are transmitted. The filtering region appears far from the carrier frequency, with a 20 dB/decade decrease of the phase noise. The cut-off frequency and the free running spectral line width are respectively of 60MHz and 1 MHz for bulk laser and of 5.5MHz and 10 kHz for QD structure. Between these two regions, the transition region can be distinguished, in which the noise is dominated here by the contribution of the free running SP laser [28, 29]. These phase noise curves also allow us to point out clearly the shorter cut-off frequency obtained with the QD laser, that leads to a better filtering effect as compared with the bulk laser. However bulk structure behavior are independent on the optical polarization. The narrow line width exhibited by these components enables the achievement of low timing-jitter in actively mode-locked lasers. All optical phase noise filtering effect is in agreement with ITU requirement and so appears to be achievable using these structures

CONCLUSION

The longitudinal mode mutual injection locking and the passive mode locking leading to self pulsation have been analyzed by using multimode rate equations Self pulsation appears to be easily achievable as observed experimentally.

The resulting optical phase correlation between the optical modes is determinant for the self pulsation phase noise. As it was observed experimentally and theoretically, the self pulsation is characterized by a large reduction of the RF spectral line width as compared to those of the optical modes involved in the beating process. Self-Pulsation at 45 GHz in the 1.5- μm monolithic single-section quantum dots Fabry-Perot semiconductor lasers, without saturable absorber, exhibits for instance a mode-beating line width lower than 100 kHz, demonstrating a high phase correlation between these modes.

The application of the self pulsating lasers to optical clock recovery shows that the free running beating spectral line width) is determinant for the recovered clock properties.

These promising results open the ways to design high performance low timing-jitter components for high bit-rate optical communications and optical signal processing.

Acknowledgement: the works presented in this paper are partly supported by French RNRT "ROTOR" project.

REFERENCE

- 1 R. Scholtz, "Frame Synchronization Techniques", IEEE Transactions on Communications, Volume 28- 8, Part 2, pp1204-1213, 1980.
- 2 L. F. Tiemeijer, P. I. Kuindersma, P. J. A. Thijs, and G. L. J. Rikken, "Passive FM locking in InGaAsP semiconductor lasers", IEEE Journal of Quantum Electronics, vol.25, pp. 1385–1392, 1991.
- 3 K. Sato, "Optical pulse generation using Fabry-Perot lasers under continuous wave operation", IEEE Journal of Selected Topics in Quantum Electronics, vol.9, pp. 1288–1293, 2003.
- 4 M. Mohrle, B. Sartorius, R. Steingruber, and P. Wolfram, "Electrically switchable self-pulsations in integratable multisection DFB-lasers", IEEE Photonics Technology Letters, vol. 8, pp. 28–30, 1996.
- 5 W. Mao, Y. Li, M. Al-Mumin, and G. Li, "All-optical clock recovery from RZ-format data by using a two-section gain-coupled DFB laser", Journal of Lightwave Technology, vol. 20, pp. 1705–1714, 2002.
- 6 S. Arahira, S. Oshiba, Y. Matsui, T. Kunii, and Y. Ogawa, "500 GHz optical short pulse generation from a monolithic passively mode-locked distributed Bragg reflector laser diode", Applied Physics Letters, vol 64, No. 15, pp. 1917–1919, 1994.
- 7 T. Ohno, R. Iga, Y. Kondo, T. Ito, T. Futura, H. Ito and K. Sato, "Wide locking-range 160-GHz optical clock recovery from 160-Gbit/s signal using mode-locked laser diode", in Proc. Optical Fiber Communication 2004, paper WD5, Los Angeles, 2004.
- 8 H. Bao, Y. J. Wen, and H. F. Liu, "Impact of saturable absorption on performance of optical clock recovery using a mode-locked multisection semiconductor laser", IEEE Journal of Quantum Electronics, vol. 40, No. 9, pp. 1177–1185, 2004.
- 9 G.-H. Duan, C. Gosset, B. Lavigne, R. Brenot, B. Thedrez, J. Jacquet, and O. Leclerc, "40 GHz all-optical clock recovery using polarization insensitive distributed Bragg reflector lasers," in Proc. Conf. Lasers and Electro-Optics, Baltimore, MD, 2003, Paper CThQ5, 2003.
- 10 T. Ohno et al.: 'A 240-GHz active mode-locked laser diode for ultrabroadband fiber-radio transmission systems'. OFC'05, Anaheim, CA, USA, Paper PDP13, 2005
- 11 A. P. Bogatov, P. G. Eliseev, and B. N. Sverdlov, "Anomalous interaction of spectral modes in a semiconductor laser," IEEE J. Quantum Electron., vol. 11, no. 7, pp. 510–515, 1975.
- 12 K. A. Shore and W. M. Yee, "Theory of self-locking FM operation in semiconductor lasers", in Proc. Inst. Elect. Eng., vol. 138, pp.91–96, 1991.
- 13 G. P. Agrawal and N. K. Dutta, "Semiconductor lasers", 2nd edition, Kluwer Academic Publishers, Chapter 6, 1993.
- 14 G. P. Agrawal, "Population pulsations and nondegenerate four-wave mixing in semiconductor lasers and amplifiers," J. Opt. Soc. Amer. B, vol. 5, no. 1, pp. 302–304, 1988.
- 15 J. Renaudier, G.-H.Duan, J.-G. Provost, H. Debregas-Sillard and P. Gallion - "Phase Correlation between Longitudinal Modes in Semiconductor Self-Pulsating DBR Lasers". IEEE Photonics Technol. Lett. PTL, 17-04, pp. 741-743, 2005.
- 16 P. Gallion, G. Debarge and C. Chabran, "Output spectrum of an unlocked optically driven semiconductor laser". Optics Lett., 22-17, pp. 294-296, 1986.
- 17 R. Adler, "A study of locking phenomena in oscillators", Proc. IRE, vol. 34, pp. 351-357, 1946.

- 18 H.L. Stower and W.H. Steiner, "locking of laser oscillators by light injection", *Appl. Phys. Lett.* 8, pp.91-93, 1966.
- 19 K. Kurokawa, "Injection locking of microwave solid-state oscillators", *Proc. IEEE*, 61, (10), pp. 1386–141, 1973
- 20 C. H. Henry "Theory of the linewidth of semiconductor lasers", *IEEE Journal of Quantum Electronics*, vol. 18, No. 2, pp.259–264, 1982.
- 21 R. Lang and K. Kobayashi, "External optical feedback effects on semiconductor laser properties," *IEEE J. Quantum Electron.*, vol. QE-16, pp. 347–355, 1980.
- 22 P. Gallion and G. Debarge, "Influence of amplitude-phase coupling on the injection locking bandwidth of a semiconductor laser", *Electron. Lett.*, 21-7, pp. 264-266, 1985
- 23 I. Petitbon, P. Gallion, G. Debarge and C. Chabran, "Locking bandwidth and relaxation oscillations of an injection-locked semiconductor laser", *Electron Lett.*, 22-17, pp. 889-890, 1986.
- 24 G. R. Gray and G. P. Agrawal, "Importance of self-induced carrier density modulation in semiconductor lasers", *IEEE Photonics Technology, Letters*, vol.4, pp. 1216–1219, 1992.
- 25 P. Landais, J. Renaudier, P. Gallion and G.-H. Duan, "Analysis of self-pulsation in distributed Bragg reflector laser based on four-wave mixing". *Proc. SPIE Vol. 5349*, p. 262-270, *Physics and Simulation of Optoelectronic Devices XII*; Marek Osinski, Hiroshi Amano, Fritz Henneberger; Eds, 2004.
- 26 H. de Belleseise. "La réception synchrone". - *Onde Electrique*, vol.11, 1932.
- 27 G.-H Duan and G. Pham "Injection-locking properties of self pulsation in semiconductor lasers" *Optoelectronics, IEE Proceedings-Volume 144*, Issue 4, Page(s): 228 – 234, 1997.
- 28 J. Renaudier, R. Brenot, B. Dagens, F. Lelarge, B. Rousseau, F. Poingt O. Legouezigou, F. Pommereau, A. Accard, P. Gallion And G-H. Duan, "45 GHz Self-Pulsation with Narrow Linewidth in Quantum Dots Fabry-Perot Semiconductor Lasers at 1.5- μm ". *Electronics Letters Volume 41*, Issue 18, pp. 1007-1008, 2005.
- 29 J. Renaudier, B. Lavigne, M. Jourdran, P. Gallion, F. Lelarge, B. Dagens, A. Accard, O. Legouezigou, G.-H. Duan, G.-H, "First demonstration of all-optical clock recovery at 40 GHz with standard-compliant jitter characteristics based on a quantum-dots self-pulsating semiconductor laser" *European Conference on Optical Communication, ECOC Sept. 2005*